

TESTING SOFT ADHESIVES WITH THE BUTT JOINT GEOMETRY

Costantino CRETON

Laboratoire de Physico-Chimie des Polymères et de la Matière Divisée
 Ecole Supérieure de Physique et Chimie Industrielle
 10, Rue Vauquelin, 75231 Paris Cédex 05, France
 email: Costantino.Creton@espci.fr

I. INTRODUCTION

A variety of adhesion tests serving different purposes have been developed in the PSA industry. However almost all of them provide the user with a single number, characteristic of performance such as the peel force or tack force or shear holding time and do not provide any insights on the underlying failure mechanisms responsible for the final result.

The probe tack test, is widely used to test the short-time, low-pressure adhesion. This test, which is effectively a test of an adhesive layer in a butt joint geometry has the advantage of applying a fairly uniform displacement (uniform stress field and strain rate) to the adhesive film over the whole surface of the probe^{1,2}, and for those soft adhesives where failure involves the formation of cavities and fibrils^{3,4}, it facilitates the analysis of the process. A set of probe-tack curves obtained for different pressure-sensitive-adhesives (PSA) and varying experimental conditions are displayed on *Figure 1*. The maximum nominal stress σ_{\max} , the maximum nominal strain ϵ_{\max} , and the adhesion energy, W_{adh} , defined as the integral under the stress-strain curves, are the easily accessible parameters characterizing the performances of a PSA in such a test, and provide clues for the practical design of the molecular structure of the polymeric material for a given application as pointed out by Zosel⁵. However, for a more refined optimization of the properties, it is helpful to understand what really happens when testing the adhesive film and how its molecular structure is involved. New developments in both instrumentation and interpretation of the results have provided insights in the debonding mechanisms of soft adhesive layers. In particular the breakdown of the debonding process in separate stages allows a better understanding of the role of the molecular features of the adhesive and the coupling between the rheological properties of the adhesive and the surface properties of the adherent. Some of these new concepts are reviewed here with the help of experimental examples.

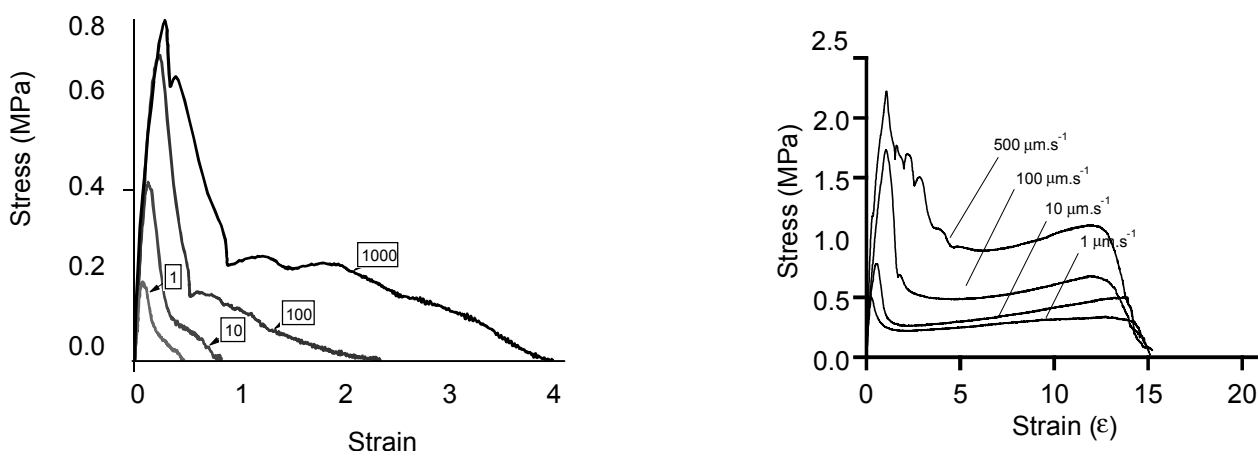


Figure 1 : stress - strain curves at room temperature as a function of debonding speed for (a) a cross-linked acrylic adhesive, and (b) a SIS based adhesive.

II. INSTRUMENTED PROBE TACK TEST

We perform the mechanical measurement as follows : the adhesive layer is deposited as a 50-100 μm thick layer on a clean glass slide, and a flat cylindrical probe, of radius 3 to 5 mm, usually made of glass or stainless steel, is brought into contact with it and subsequently removed as shown on *Figure 2*. If desired, the surface of the probe can be coated with a molecularly thin mineral or organic layer (soft/hard polymer...) in order to modify surface interactions. During the compression phase, we apply a nominal contact pressure of 1 MPa, in order to achieve a maximum contact area. The contact time can be varied between 1 sec and more than 1 hour, and the probe is then removed from the film at a constant probe velocity which can be varied between 1 and 1000 $\mu\text{m/s}$. The temperature is controlled, and can be varied between -20°C and 60°C . Our custom-designed probe tack apparatus allows the observation of the adhesive film from underneath the transparent substrate with a microscope and/or a video camera along with the simultaneous acquisition of a nominal stress and strain curves. The nominal stress σ , is defined as the force divided by the contact area, and the strain ϵ , is defined as the displacement divided by the thickness of the film. Details on the experimental setup can be found elsewhere⁶.

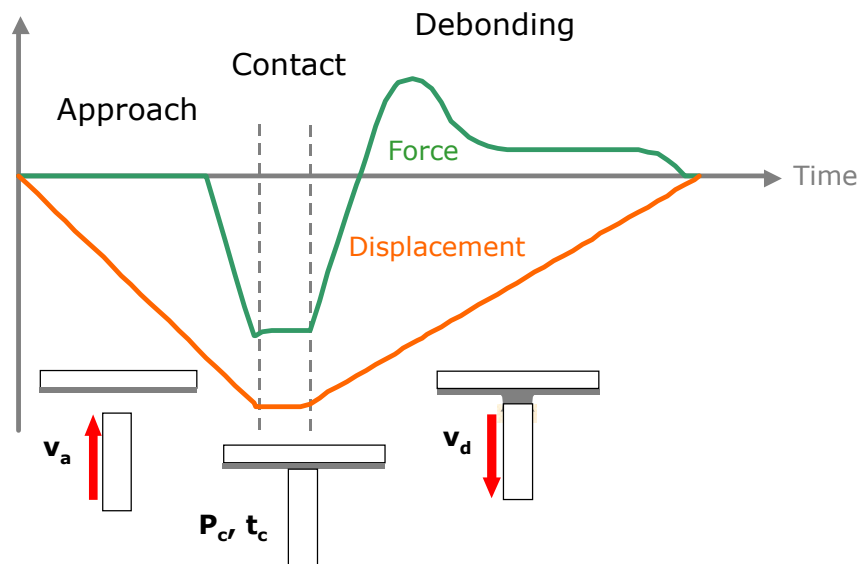


Figure 2 : schematic of a probe-tack test

The key advantage of the probe test is the possibility to break up the debonding process into separate stages, which are described schematically in *Figure 3* :

1. Homogeneous expansion.
2. Initiation of the failure process at low deformation through the formation of microscopic cavities at the interface between the film and the probe or in the bulk of the adhesive layer. The load-bearing area decreases, and as a direct consequence, σ goes through a maximum, defining σ_{max} .
3. Expansion of these cavities, mostly in the lateral dimensions.
4. Elongation of the walls in between the cavities in the direction of the applied stress, at an approximately constant level of nominal stress. Eventually fracture occurs by creeping (cohesive failure) or debonding of the foot of the polymer ligament from the probe, defining ϵ_{max} .

The details of each one of these individual stages (levels of stress, strain, shape of the curve) are sensitive to the rheological properties of the adhesive and to the surface properties of the probe. However different properties influence different stages and it is the purpose of this paper to provide interpretation keys.

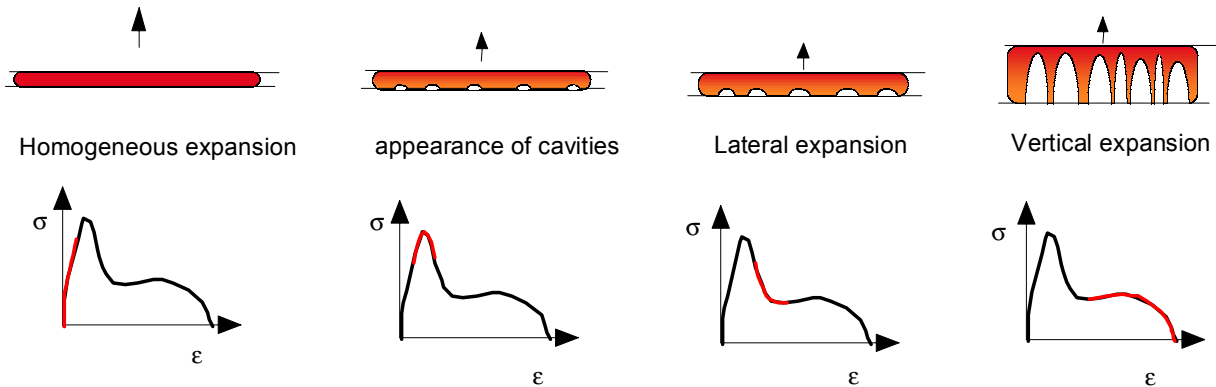


Figure 3: Typical debonding mechanisms observed during a probe test on a soft adhesive

III. MECHANICAL ANALYSIS AND EXPERIMENTAL RESULTS

The first mechanism occurring during the application of the tensile stress is the formation of a cavity. The underlying reasons for the occurrence of this cavitation process have been recently discussed^{2,7,8} and can be summarized as follows:

The most common way for a material to release its elastic strain energy when it is stressed in tension, is to initiate and then propagate a crack. For soft adhesives, i.e. polymer melts or gels of low elastic modulus, this process is not favoured as it requires large bulk viscoelastic dissipations and the available strain elastic energy is not very large⁷. Moreover, in the probe tack geometry, the lateral dimensions of the compliant adhesive layer, i.e. diameter of the probe, are significantly larger than its thickness, h . Consequently, as the layer is deformed in the thickness direction, lateral strains cannot be accommodated and significant lateral stresses develop. The resulting strong hydrostatic pressure induces an alternative deformation mode to the propagation of a crack, namely the cavitation process⁷.

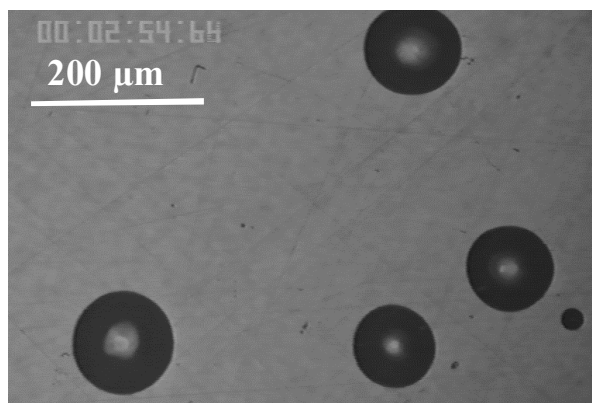


Figure 4: Video capture of cavities at the interface between the probe surface and the adhesive layer for an SIS based adhesive.

Figure 4 shows a magnified video capture of cavities for a styrene-isoprene-styrene (SIS) based PSA on a steel surface, observed with a microscope working in reflection mode. Focusing

was done on the surface of the polished steel surface probe. When cavities appear as a result of the applied tensile stress, they are sharply outlined, implying therefore that, in this case, nucleation occurred at / or very near the interface, and expanded both in the bulk of the adhesive layer and at the interface. Many years ago, it was noted by Gent⁹ that a cross-linked elastomer could not sustain a hydrostatic stress higher than approximately its elastic modulus without undergoing cavitation, that is the unstable expansion of an existing defect into a macroscopic visible cavity. This mechanical analysis was extended to a polymer melt by considering its time dependent modulus¹⁰. For a polymer melt, the rapid growth of a cavity is predicted when :

$$\sigma_{hyd} > E(t) \quad (1)$$

where $E(t)$ is the time dependent elastic modulus and σ_{hyd} is the hydrostatic component of the applied stress. In agreement with Kaelble predictions⁷, and applying time-temperature superposition, we indeed observed a direct correlation between the shear elastic modulus $G'(\omega)$ and the maximum stress σ_{max} (V_{deb}) for different model acrylic PSA's over a large range of frequency / debonding rates and temperatures⁶. An increase in σ_{max} with an increasing rate of debonding or a decreasing temperature was observed, and that increase closely matched the increase of the elastic component of the shear modulus $G'(\omega)$, as shown on *Figure 5*. This result was found on other adhesives although the ratio σ_{max}/G' was not identical from one adhesive to another.

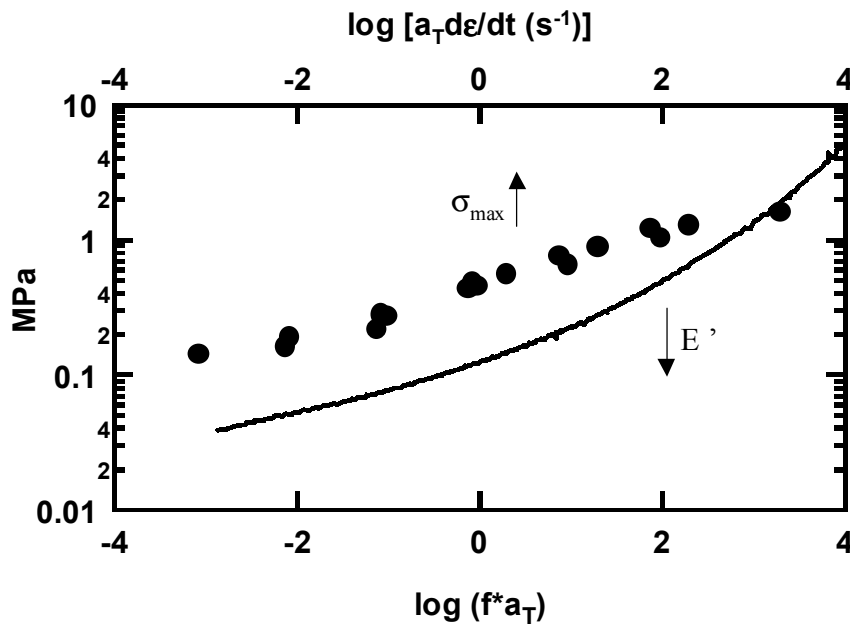


Figure 5: σ_{max} and E' as a function of the reduced shear frequency $a_T f = \omega/2\pi$, where a_T is the WLF shift factor, or of the reduced strain rate $a_T d\epsilon/dt$. (●) σ_{max} ; (---) E'

Therefore the value of σ_{max} in a probe test provides us chiefly information on the elastic bulk properties of the adhesive rather than on its adhesive properties.

However, intuitively, the probe surface roughness should also impact the cavitation process, since air bubbles could be trapped at the interface or an inhomogeneous strain field could be created from asperities on the surface. Both could act as nucleation sites for the formation of cavities. Such effects are observed for example, when the roughness of the probe is varied. Recent systematic experiments have shown that the amplitude of the surface asperities has a direct effect on the level of stress at which the cavities are formed¹¹. The rougher surface giving a much lower value of σ_{max} than the very smooth one.

Once a few cavities have appeared and as the adhesive film is further strained in the tensile direction, the next process is usually the lateral growth of existing cavities. This lateral growth is always accompanied by a decrease of the force on the probe mostly due to the decrease in load-bearing area that this process entails. This lateral growth, essentially an interfacial process, as opposed to the nucleation of the cavities, is analogous to the propagation of a crack and can be analyzed with similar tools. When a crack propagates at the interface between a rigid surface and an elastomer, there is a relationship between the elastic energy which is released ahead of the crack (\mathcal{G}) and the crack velocity. This relationship which is strictly valid when the elastomer is fully elastic can be given by an equation of the type^{12,13}:

$$\mathcal{G} = \mathcal{G}_o (1 + (v/v^*)^n) \quad (2)$$

where \mathcal{G}_o is the value of the energy release rate at a vanishing crack velocity (which can sometimes be equated to the thermodynamic work of adhesion of the polymer melt on the surface) and the parameters v^* and n characterize the velocity dependence arising from viscoelastic dissipation in the vicinity of the crack tip. Although equation 2 cannot be applied directly in the confined geometry of a probe-tack test or for very viscoelastic materials, it gives an insight into the type of coupling existing between the rheological properties of the adhesive and the surface properties of the adherent¹⁴. \mathcal{G}_o , for typical PSA's on steel surfaces, is rather high and prevents extensive lateral crack propagation, favoring the formation of a fine bubble structure and subsequent fibril stretching mechanism. Insight on the nature of the coupling can however be obtained from studies on model systems.

Substantial changes in \mathcal{G}_o can be induced by varying the surface probe chemistry, for example by coating a steel surface with a thin layer of poly(dimethyl siloxane) (PDMS). In this case, \mathcal{G}_o is low for most PSA's, the cavities grow mainly at the interface and their coalescence lead to a rapid adhesive failure^{14,15}. An example of the change in failure mechanism due to the reduction of \mathcal{G}_o is given on *figure 6*. Alternatively, a change in the dissipative rheological properties of the adhesive layer (G'') will affect the dissipative part of equation 2 and therefore v^* and n . One should therefore stress that this lateral propagation stage is the main source of interfacial information. A modification of the adhesive interactions or of the dissipative properties of the adhesive will have its most important effect on the decrease in force after the maximum.

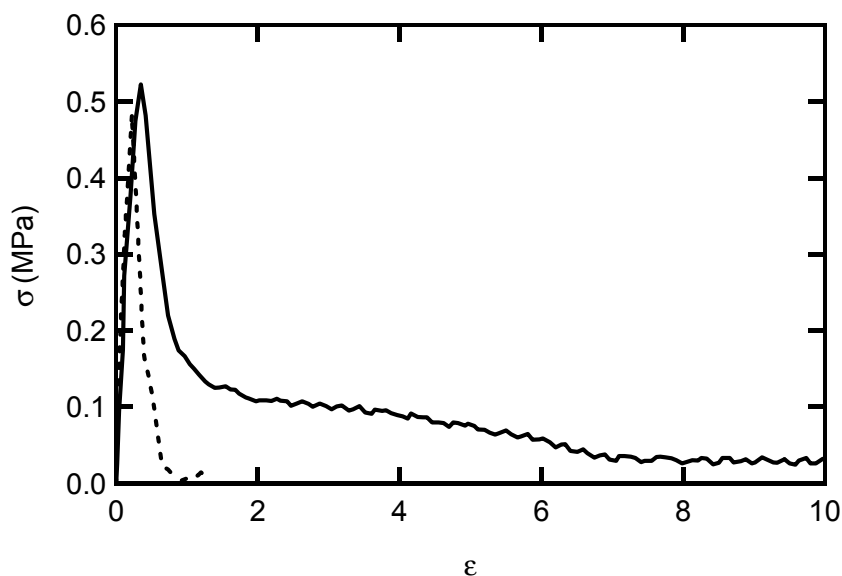


Figure 6: Stress-strain curves of a soft adhesive on steel (solid line) and on a PDMS coated surface (dashed line). Note the rapid decrease in stress after the maximum for the PDMS surface compared to steel, while the two values of σ_{max} are almost identical.

Finally, if the lateral propagation is slow, the individual cavities/cracks will never coalesce and the walls between cavities will extend in the direction perpendicular to the plane of the film. This vertical elongation of the walls between cells implies that, at the molecular scale, there is a progressive orientation of the polymer chains in the direction of traction^{4,16}. Some of the extensional growth is a result of a creeping process and some is due to the drawing of unoriented polymer from the film. The respective importance of the two mechanisms will depend on the rheological properties of the adhesive in elongation (large strain regime). Although the elongational properties of a polymer melt of linear chains can be reasonably well predicted by its linear viscoelastic properties, this is not the case for the partially crosslinked gels used normally as PSA¹⁷. For example, *Figure 7* shows stress-strain curves for a SIS based PSA with a variable amount of SI diblock¹⁸. It is clear that the fibrillar part of the curve at large strain is more affected than the value of σ_{max} .

In this case, the ultimate failure occurs by detachment of the foot of the fibril from the surface of the adherent, while for a weakly strain hardening acrylic adhesive or for an acrylic polymer melt, some cohesive fracture of the fibrils could be observed^{6,19}.

The maximum extension achieved, and therefore the adhesion energy, depend as a result strongly on the elongational properties of the adhesive and weakly on the interfacial strength still characterized by G_0 .

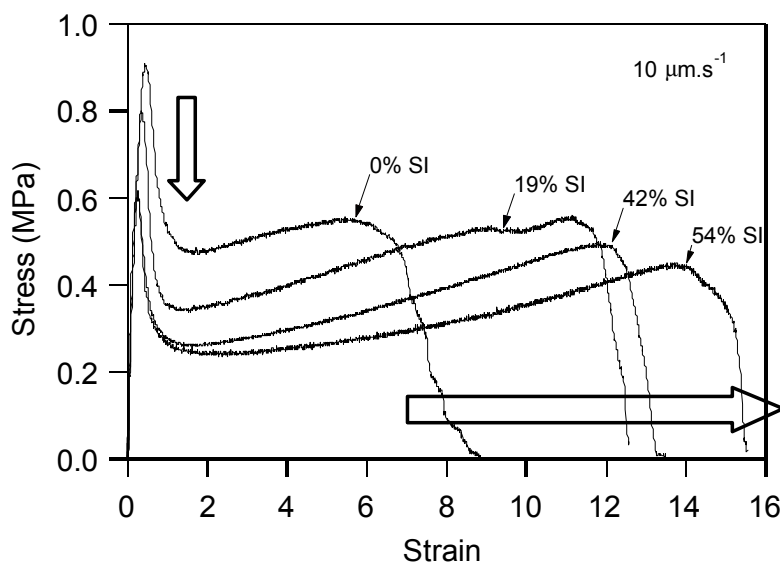


Figure 7: Stress-strain curves of four adhesives based on SIS+SI. The increasing proportion of SI in the adhesive significantly modifies the fibrillation part of the curve. This difference is captured best by the elongational properties of the adhesives. $T = 22^{\circ}\text{C}$, Probe debonding velocity = $10\mu\text{m/s}$.

V. CONCLUSION

The performance of PSA's is critically dependent on the fine control of their yielding behavior under relatively small stresses. This yielding behavior often occurs in highly confined geometries, and the ability to design tests with realistically large values of the confinement ratio is one of the advantages of the probe tack test. Moreover, because of the uniform strain and strain rate which are applied by a flat probe test, the debonding process can be easily broken down into more elementary steps and analyzed. As opposed to a more conventional test such as peel, an instrumented tack test provides information on the sensitivity of each specific step to the molecular features and experimental conditions.

In particular we have been able to distinguish between the initiation of failure (controlled by the linear viscoelastic G'), the interfacial propagation of a crack (controlled by G_c) and the extension of a fibril (controlled by the nonlinear extensional properties of the adhesive).

REFERENCES

- (1) Creton, C.; Lakrout, H. *J. Polym. Sci. B Polym. Phys.* **2000**, *38*, 965-979.
- (2) Lin, Y. Y.; Hui, C. Y.; Conway, H. D. *J. Polym. Sci. B Polym. Phys.* **2000**, *38*, 2769-2784.
- (3) Zosel, A. *Adv. Pressure Sensitive Adhes. Technol.* **1992**, *1*, 92-127.
- (4) Creton, C. *Materials Science of Pressure-Sensitive-Adhesives*; 1st ed.; Meijer, H. E. H., Ed.; VCH: Weinheim, 1997; Vol. 18, pp 707-741.
- (5) Zosel, A. *Colloid Polym. Sci.* **1985**, *263*, 541-553.
- (6) Lakrout, H.; Sergot, P.; Creton, C. *J. Adhes.* **1999**, *69*, 307-359.
- (7) Crosby, A. J.; Shull, K. R.; Lakrout, H.; Creton, C. *J. Appl. Phys.* **2000**, *88*, 2956-2966.
- (8) Chikina, I.; Gay, C. *Phys. Rev. Lett.* **2000**, *85*, 4546-4549.
- (9) Gent, A. N.; Lindley, P. B. *Proc. Roy. Soc. London, A* **1958**, *249 A*, 195-205.
- (10) Kaelble, D. H. *Trans. Soc. Rheol.* **1971**, *15*, 275-296.
- (11) Chiche, A.; Pareige, P.; Creton, C. *C.R. Acad. Sci. Paris, IV* **2000**, *1*, 1197-1204.
- (12) Ahn, D.; Shull, K. R. *Langmuir* **1998**, *14*, 3646-3654.
- (13) Maugis, D.; Barquins, M. *J. Phys. D: Appl. Phys.* **1978**, *11*, 1989-2023.
- (14) Creton, C.; Hooker, J. C.; Shull, K. R. *Langmuir* **2001**, *17*, 4948-4954.
- (15) Josse, G.; Creton, C.; Dorget, M., Proceedings of Euradh 2000; Lyon; 2000, pp 165-169.
- (16) Good, R. J.; Gupta, R. K. *J. Adhes.* **1988**, *26*, 13-36.
- (17) Christensen, S. F.; Flint, S. C. *J. Adhes.* **2000**, *72*, 177-207.
- (18) Roos, A.; Creton, C., Proceedings of 25th Annual Meeting of the Adhesion Society; Orlando; 2002, pp 371-374.
- (19) Lakrout, H.; Creton, C.; Ahn, D.; Shull, K. R. *Macromolecules* **2001**, *34*, 7448-7458.